

Transitions between symmetric and asymmetric solitons in dual-core systems with cubic-quintic nonlinearity

Lior Albuch and Boris A. Malomed

*Department of Interdisciplinary Studies, School of Electrical Engineering,
Faculty of Engineering, Tel Aviv University, Tel Aviv 69978, Israel*

It is well known that a symmetric soliton in coupled nonlinear Schrödinger (NLS) equations with the cubic nonlinearity loses its stability with the increase of its energy, featuring a transition into an asymmetric soliton via a subcritical bifurcation. A similar phenomenon was found in a dual-core system with quadratic nonlinearity, and in linearly coupled fiber Bragg gratings, with a difference that the symmetry-breaking bifurcation is supercritical in those cases. We aim to study transitions between symmetric and asymmetric solitons in dual-core systems with saturable nonlinearity. We demonstrate that a basic model of this type, *viz.*, a pair of linearly coupled NLS equations with the cubic-quintic (CQ) nonlinearity, features a *bifurcation loop*: a symmetric soliton loses its stability via a supercritical bifurcation, which is followed, at a larger value of the energy, by a reverse bifurcation that restores the stability of the symmetric soliton. If the linear-coupling constant λ is small enough, the second bifurcation is subcritical, and there is a broad interval of energies in which the system is *bistable*, with coexisting stable symmetric and asymmetric solitons. At larger λ , the reverse bifurcation is supercritical, and at very large λ the bifurcation loop disappears, the symmetric soliton being always stable. Collisions between solitons are studied too. Symmetric solitons always collide elastically, while collisions between asymmetric solitons turns them into breathers, that subsequently undergo *dynamical symmetrization*. In terms of optics, the model may be realized in both the temporal and spatial domains.

PACS numbers: 05.45.Yv; 42.65.Tg; 42.70.Nq

I. INTRODUCTION

Twin-core nonlinear fibers and waveguides (alias *couplers*) have been a subject of considerable interest in nonlinear optics and, more generally, in nonlinear-wave theory since the pioneering works by Jensen and Maier [1], who introduced the model of a dual-core nonlinear optical fiber. In particular, many papers analyzed dynamics of solitary waves in models of nonlinear couplers (see, e.g., review [3] and Ref. [4]), although such solitons have not yet been created in the experiment.

It has been known for a long time [2] that a symmetric soliton in the model of the twin-core fiber, with its energy equally divided between the cores, becomes unstable when the energy exceeds a certain critical value. Then, it was found that this instability gives rise to a *pitchfork bifurcation*: a pair of new, stable *asymmetric solitons* (which are mirror images to each other) appear when the symmetric state loses its stability [6]. This bifurcation was studied in detail by means of numerical [7, 8] and analytical [8] methods (the latter was based on the variational approximation, see Section 6 of review [9]), with a conclusion that the bifurcation is slightly *subcritical*, according to the standard definition [10]. Namely, new stable asymmetric states appear at a value of the soliton's energy which is slightly smaller than that at which the symmetric soliton becomes unstable, thus giving rise to the *bistability* (coexistence of stable symmetric and asymmetric solitons) in a narrow interval of energies before the pitchfork bifurcation.

The studies of solitons in nonlinear dual-core systems were extended in various directions. First, the change of the character of the bifurcation was investigated in a practically interesting case of a dual-core nonlinear optical fiber with asymmetric cores [8, 11]. Further, four-component solitons were considered in a more sophisticated model, which takes into regard two orthogonal polarizations of light in the dual-core fiber [12]. Then, bifurcations breaking the symmetry of two-component solitons were studied in a symmetric dual-core nonlinear fiber with the Bragg grating carried by each core [13], and in a system of parallel-coupled waveguides with the quadratic, $\chi^{(2)}$ (rather than cubic, $\chi^{(3)}$), nonlinearity [14]. In the two latter cases, the symmetry-breaking bifurcation was found to be supercritical, rather than subcritical (i.e., the destabilization of the symmetric soliton immediately gives rise to a pair of stable asymmetric ones, without the bistability). In addition, three-component solitons and their bifurcations were studied in a system of three linearly-coupled fibers forming a triangular configuration [15], as well as in a similar configuration formed by three Bragg gratings [16].

A universal feature of all the above-mentioned systems is that the symmetric soliton is destabilized with the increase of its energy, as the self-focusing nonlinearity favors states in which a larger part of the energy is concentrated in one core (which is explained by the fact that the part of the system's Hamiltonian accounting for the nonlinearity tends to be lower in such an asymmetric configuration than in its symmetric counterpart). Past the symmetry-breaking bifurcation point, the asymmetry of the energy distribution between the cores increases monotonously with the further

increase of the total energy.

However, the self-focusing nonlinearity may feature saturation with the increase of the power in some optical media. In particular, it was inferred from experimental data that nonlinearity of chalcogenide glasses [17] and some organic transparent materials [18] is adequately approximated by adding a self-defocusing $\chi^{(5)}$ (quintic) term to the self-focusing $\chi^{(3)}$ one. The respective *cubic-quintic* (CQ) nonlinearity furnishes a paradigmatic example of the saturation, as well as of the competition between self-focusing and self-defocusing nonlinearities [19].

A model of a dual-core optical fiber or waveguide with saturable nonlinearity is an interesting object in its own right, and may also be relevant for applications to all-optical switching. In particular, the symmetry-breaking bifurcation between continuous-wave (CW) states (rather than solitons) in a model of a coupler with saturable nonlinearity was considered long ago in Ref. [20], with a conclusion that the bifurcation is subcritical in this case. However, CW states in couplers with a self-focusing nonlinearity are always subject to modulational instability [21], therefore it is necessary to consider solitons, rather than the CW. Qualitatively new features may be expected in such systems. Indeed, since the spontaneous symmetry breaking of soliton states, observed at energy exceeding the critical value, is accounted for by the trend to concentrate a larger part of the energy in one core with the growing strength of the self-focusing, the saturation, which *attenuates* the self-focusing with the further increase of the energy, should eventually give rise to a reverse trend. Thus, a *reverse bifurcation* may occur in the system, restabilizing the symmetric soliton and eliminating asymmetric states.

This work aims is to produce a full picture of bifurcations in the symmetric dual-core system with the CQ nonlinearity. In Section II, we introduce the model, whose single free parameter is the constant λ of the linear coupling between the cores. Main results are presented in Section III: if λ is smaller than a certain value λ_{\max} , the system features a *bifurcation loop*, first destabilizing and then restabilizing the symmetric soliton, as may be expected (see above). The direct (symmetry-breaking) bifurcation is always supercritical, while the reverse one is subcritical (featuring a large bistability region, which may be of considerable interest to applications [2] - [4]), except for a narrow interval near $\lambda = \lambda_{\max}$, where the reverse bifurcation is supercritical, without the bistability. The loop disappears at $\lambda = \lambda_{\max}$; in the region of $\lambda > \lambda_{\max}$, the symmetric soliton is always stable, while asymmetric ones do not exist. Direct simulations demonstrate that the stability of all soliton branches exactly complies with what may be expected from general principles of the bifurcation theory [10].

In Section IV, we additionally investigate collisions between moving solitons, which a natural issue to address as the Galilean invariance of the model allows one to generate moving solitons. We infer from simulations that collisions between stable symmetric solitons are completely elastic, while asymmetric solitons collide inelastically and separate after the collision in the form of breathers. Conclusions are formulated in Section V.

II. THE MODEL

Linearly coupled CQ nonlinear Schrödinger (NLS) equations for the amplitudes u and v of the electromagnetic fields propagating along the coordinate z in the two cores of an optical waveguide can be cast in a normalized form,

$$iu_z + u_{\tau\tau} + 2|u|^2u - |u|^4u + \lambda v = 0, \quad (1)$$

$$iv_z + v_{\tau\tau} + 2|v|^2v - |v|^4v + \lambda u = 0, \quad (2)$$

where $\tau \equiv t - z/V_0$ is the local time (V_0 is the group velocity of the carrier wave). The model assumes anomalous group-velocity dispersion, GVD (otherwise it will generate no bright solitons), whose coefficient is normalized to be 1. The coefficients in front of the self-focusing $\chi^{(3)}$ and self-defocusing $\chi^{(5)}$ terms can always be normalized as set in Eqs. (1) and (2), the only remaining irreducible parameter of the model being the linear-coupling constant λ (we define it to be positive), that determines a characteristic coupling length, $z_{\text{coupl}} \sim 1/\lambda$ (in real couplers, z_{coupl} takes values from ~ 1 mm up to ~ 1 cm, in physical units). In nontrivial soliton states (those which are essentially affected by the linear coupling), the characteristic nonlinearity and dispersion lengths, z_{nonlin} and z_{disp} , must match z_{coupl} . The successful creation of solitons in fiber Bragg gratings, with the nonlinearity length $\lesssim 1$ cm [22], suggests that z_{nonlin} for high-power pulses in silica fibers can indeed be brought down to the necessary size, in the range of 1 mm – 1 cm (the nonlinearity length is determined by the core itself, rather than by its coupling to another core or grating written on its surface). On the other hand, while the intrinsic GVD of the fiber waveguide may not be sufficient to provide for the necessarily small z_{disp} , the effective GVD may be enhanced by several orders of magnitude by means of the same grating [22].

In addition to the above-mentioned interpretation in the *temporal domain*, the model based on Eqs. (1) and (2) may also be realized in terms of the light transmission in the *spatial domain*. In that case, the temporal variable τ is replaced by the transverse coordinate x , and the equations govern the spatial evolution of amplitudes of the electromagnetic field in a pair of parallel tunnel-coupled planar waveguides, the terms u_{xx} and v_{xx} accounting for the

transverse diffraction of light (in the usual paraxial approximation). Launching the beams with the transverse width $\Delta x \sim 20$ wavelengths (if the latter is taken, as usual, in a ballpark of $\lambda \simeq 1 \mu\text{m}$; note that the paraxial approximation is relevant for $\Delta x \sim 20\lambda$) will provide for a value of the diffraction length, $z_{\text{diff}} = 4\pi(\Delta x)^2/\lambda$, in the above-mentioned range of 1 mm – 1 cm, where it can be matched to the coupling length (for the parallel planar waveguides, z_{coupl} is essentially the same as for the dual-fiber system).

The starting point of analysis is a well-known exact soliton solution of the single CQ NLS equation [23], to which Eqs. (1) and (2) reduce in the symmetric case:

$$u = v = e^{ikz} U_{\text{symm}}(\tau),$$

$$U_{\text{symm}}(\tau) = \sqrt{\frac{2(k-\lambda)}{1 + \sqrt{1 - 4(k-\lambda)/3} \cosh(2\sqrt{k-\lambda}\tau)}}, \quad (3)$$

where the propagation constant k takes values in the interval $\lambda < k < \frac{3}{4} + \lambda$. In more sophisticated settings, solutions for a single equation with the CQ nonlinearity can be found in a numerical form. An example relevant to the spatial-domain model is a solution for the semi-nonlinear equation, with an overall nonlinear coefficient (one in front of both the cubic and quintic terms) present in the region of $x > 0$ and vanishing at $x < 0$ [24].

Following the analysis of coupled NLS equations with the $\chi^{(3)}$ nonlinearity [7, 8], we look for asymmetric stationary solutions to Eqs. (1) and (2) in the form of

$$\{u(z, \tau), v(z, \tau)\} = e^{ikz} \{U(\tau), V(\tau)\}. \quad (4)$$

If the functions U and V are complex,

$$\{U(\tau), V(\tau)\} = \{a(\tau)e^{i\phi(\tau)}, b(\tau)e^{i\psi(\tau)}\}, \quad (5)$$

with real amplitudes and phases $\{a, b\}$ and $\{\phi, \psi\}$, a straightforward corollary of the equations is the following relation, valid for localized solutions (see details in Appendix):

$$a^2 \dot{\phi} + b^2 \dot{\psi} = 0, \quad (6)$$

with the overdot standing for $d/d\tau$. For symmetric solitons, with $a = b$ and $\phi = \psi$, Eq. (6) implies, as usual, that all solutions are real. While the same is not obvious for asymmetric solitons, we demonstrate in Appendix that asymmetric complex solutions for $U(\tau)$ and $V(\tau)$ with a nontrivial phase structure cannot be generated by a bifurcation from the symmetric soliton (3). For this reason, in what follows below we consider real stationary solutions for U and V , hence the substitution of expressions (4) in Eqs. (1) and (2) leads to a system

$$\frac{d^2 U}{d\tau^2} - kU + \lambda V + 2U^3 - U^5 = 0, \quad (7)$$

$$\frac{d^2 V}{d\tau^2} - kV + \lambda U + 2V^3 - V^5 = 0. \quad (8)$$

We solved Eqs. (7) and (8) numerically by means of the finite-difference method. In this paper, we only aim to search for fundamental solitons, which correspond to even single-humped solutions to these equations. Stability of the analytical symmetric solutions (3) and asymmetric ones found in the numerical form was tested by direct simulations of Eqs. (1) and (2), performed by means of the split-step method.

Note that Eqs. (1) and (2) conserve the total energy (norm) of the solution,

$$N = \frac{1}{2} \int_{-\infty}^{+\infty} [|u(\tau)|^2 + |v(\tau)|^2] d\tau \quad (9)$$

(in the spatial-domain optical model, the norm has the physical meaning of the total power of the beams), together with the momentum and Hamiltonian (that will not be used below). For exact solutions (3), the norm is

$$N_{\text{symm}} = \frac{\sqrt{3}}{2} \ln \left(\frac{\sqrt{3} + 2\sqrt{k-\lambda}}{\sqrt{3} - 2\sqrt{k-\lambda}} \right). \quad (10)$$

It is worthy to note that expression (10) satisfies the condition $dN/dk > 0$, which, according to the known Vakhitov-Kolokolov (VK) criterion [25], is necessary for stability of the soliton family (the validity of this criterion was established, in a general form, for single-component NLS equations [26]). The VK criterion guarantees the absence of unstable modes of small perturbations with a real instability growth rate, but it does not tell anything about modes corresponding to complex eigenvalues.

III. THE BIFURCATION DIAGRAM

Symmetry-breaking bifurcation points of Eqs. (7) and (8) (critical values of k for given λ) may be looked for by adding an infinitesimal antisymmetric perturbation, $W(\tau)$, to the symmetric soliton, $\{U(\tau), V(\tau)\} = U_{\text{symm}}(\tau) \pm W(\tau)$. The substitution of this in Eqs. (7) and (8) and linearization with respect to W lead to a linear Schrödinger equation for W ,

$$-(\lambda + k)W = -\frac{d^2 W}{d\tau^2} + U_{\text{eff}}(\tau)W, \quad (11)$$

with an effective potential

$$U_{\text{eff}}(\tau) \equiv U_{\text{symm}}^2(\tau) [5U_{\text{symm}}^2(\tau) - 6]. \quad (12)$$

The first problem is to find values of k at which an even localized state appears among solutions of Eq. (11). In the model with the cubic nonlinearity only, Eq. (12) yields the effective potential $-6(k - \lambda)\text{sech}^2(\sqrt{k - \lambda}\tau)$, which is integrable, as is known from quantum mechanics. Therefore, the (single) bifurcation point in the model of the coupler with the cubic nonlinearity could be found exactly [2]. In terms of the norm of the symmetric soliton, it is $N_{\text{cubic}}^{(\text{bif})} = 2\sqrt{2\lambda/3}$. However, the effective potential in the CQ model, given by Eqs. (12) and (3), is far from being integrable, therefore we will identify bifurcation points by numerical methods.

Numerical solution of stationary equations (7) and (8) produces a sequence of bifurcation diagrams displayed in Figs. 1 and 2. In these diagrams, the soliton's *asymmetry parameter*,

$$\epsilon \equiv \frac{U_{\text{max}}^2 - V_{\text{max}}^2}{U_{\text{max}}^2 + V_{\text{max}}^2}, \quad (13)$$

where U_{max} and V_{max} are the amplitudes of the two components of the soliton, is shown versus the norm N . Note that the soliton's propagation constant k varies along with N (not shown in the diagrams).

As expected, Figs. 1 and 2 demonstrate *bifurcation loops*. The loop exists at $\lambda \leq \lambda_{\text{max}} \approx 0.44$ (in fact, the full loop was found for $\lambda \geq 0.10$, as for smaller λ it was difficult to close the loop, due to its very large size; indeed, for $\lambda \rightarrow 0$, the loop extends to $N \rightarrow \infty$, as one then has an obvious stable asymmetric solution, with $u \neq 0$ and $v = 0$, for any N). The direct (symmetry-breaking) bifurcation is observed to be always supercritical, while the reverse one, which closes the loop, is subcritical (giving rise to the bistability and concave shape of the loop, on its right side) up to $\lambda \approx 0.40$. In a narrow interval of $0.40 < \lambda < 0.44$, the reverse bifurcation is supercritical, and the (small) loop has a convex form.

It is relevant to mention that a somewhat similar sequence of bifurcation loops was reported for (modulationally unstable) CW states, rather than solitons, in a symmetric dual-core model by Snyder *et al.* [20] [see Figs. 10(a) and 10(b) in that paper]. However, that sequence was found in a model with a saturable, rather than cubic-quintic, nonlinearity in each core.

The global picture of the bifurcations is additionally illustrated by Figs. 3 and 4. They display, versus λ , the value of the asymmetry parameter (13) for the most asymmetric soliton generated by the bifurcation for given λ , and values of norm N of the symmetric soliton at points of the direct and reverse bifurcations.

Stability and instability of different branches of soliton solutions can be anticipated on the basis of general principles of the bifurcation theory [10]: the symmetric solution becomes unstable after the direct supercritical bifurcation, and asymmetric solutions emerge as stable ones at this point; after the reverse bifurcation, the symmetric solution is stable again. In the case when the reverse bifurcation is subcritical and, accordingly, the bifurcation loop is concave on its right side, two branches of asymmetric solutions (one stable and one unstable) meet and terminate at each turning point through the saddle-node (alias tangent) bifurcation; accordingly, the branches of the asymmetric solitons which terminate at the reverse-bifurcation point are unstable.

These expectations are fully borne out by direct numerical simulations. In particular, the simulations clearly demonstrate that a small symmetry-breaking perturbation triggers spontaneous rearrangement of presumably unstable symmetric solitons into stable asymmetric ones. The transition (not shown here) is accompanied by relatively small radiative loss.

Simulations of the evolution of perturbed unstable solitons, corresponding to the intermediate branches in Figs. 1 and 2 (i.e., in the case of the bistability), demonstrate that the unstable soliton, which has a choice to transform itself into either a still more asymmetric soliton, or a symmetric one, both of which are stable, clearly follows the latter route, even if the initial perturbation acted in the opposite direction, trying to make the soliton less asymmetric (not shown here in detail). In this case, the transition entails a larger radiative loss.

The instabilities of symmetric and asymmetric solitons are qualitatively different: as said above, the symmetric solutions (3) are stable according to the VK criterion, i.e., their instability may only be oscillatory [accounted for by

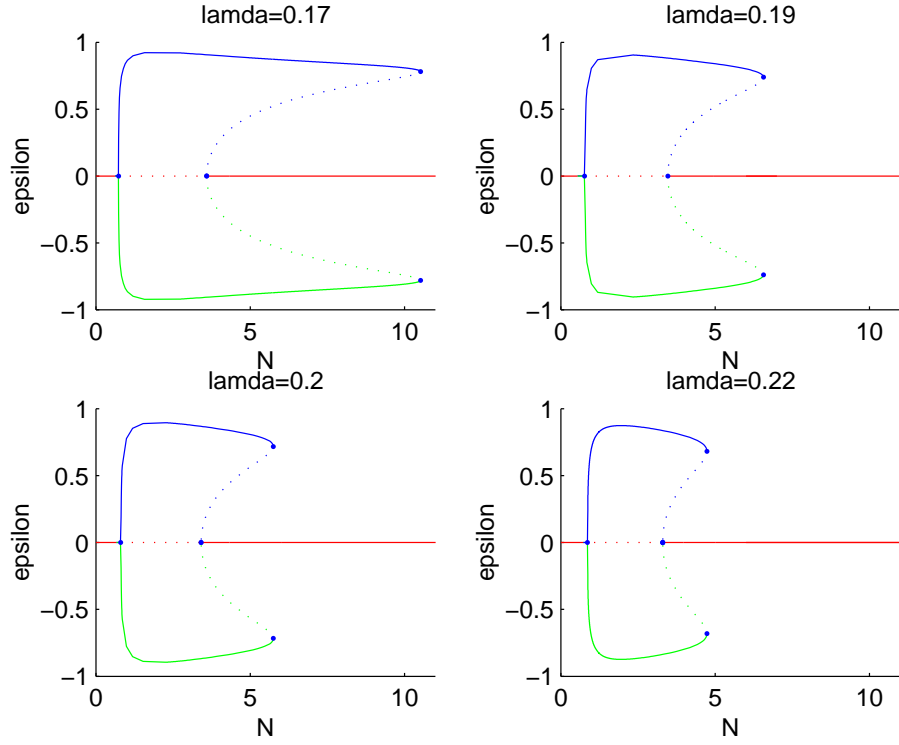


FIG. 1: A set of bifurcation diagrams for symmetric and asymmetric solitons, in the plane (N, ϵ) , as found from numerical solution of Eqs. (7) and (8) at different values of the linear-coupling constant λ . Stable and unstable branches of the solutions are shown by solid and dashed curves, respectively, and bold dots indicate bifurcation points.

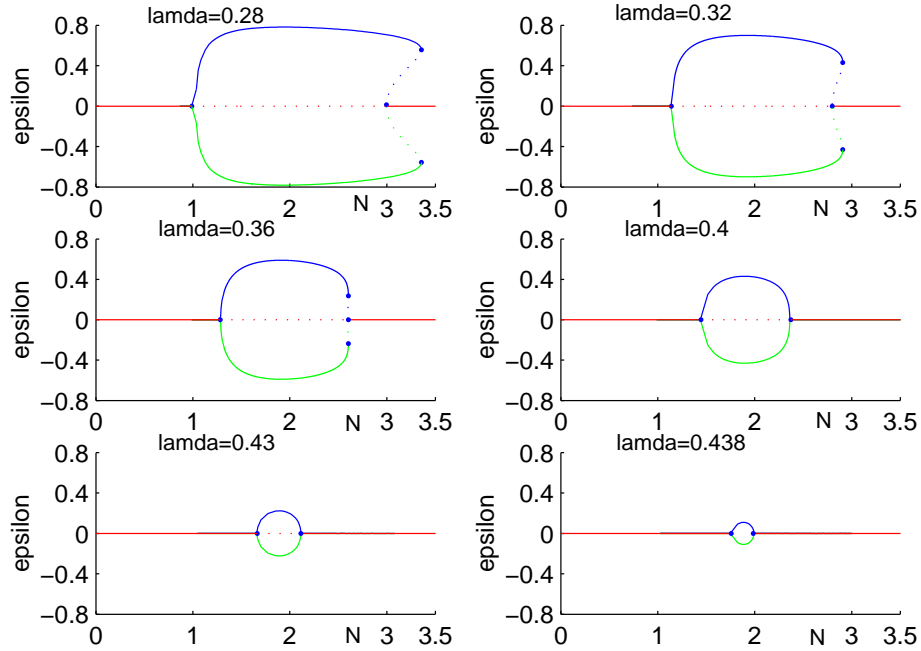


FIG. 2: Continuation of Fig. 1.

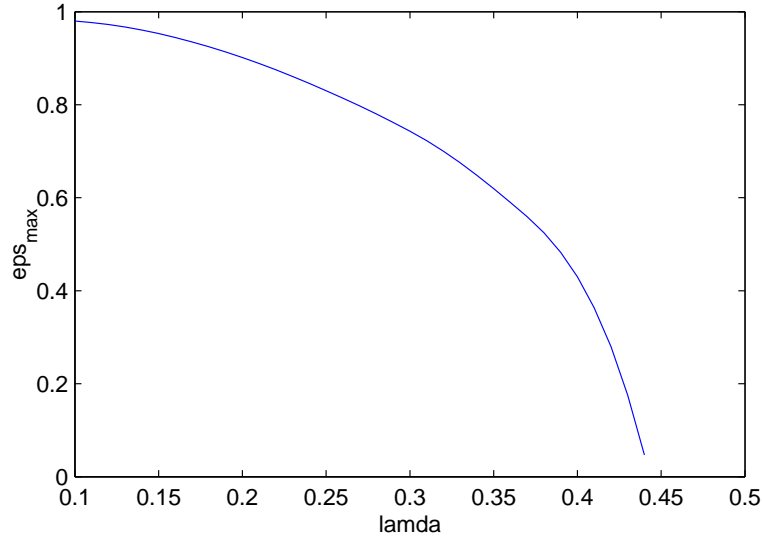


FIG. 3: The maximum value of the asymmetry parameter (13) of solitons generated by the bifurcation, versus the linear-coupling constant λ . For very small values of λ , ϵ_{\max} is not shown because of difficulties with convergence of the numerical scheme.

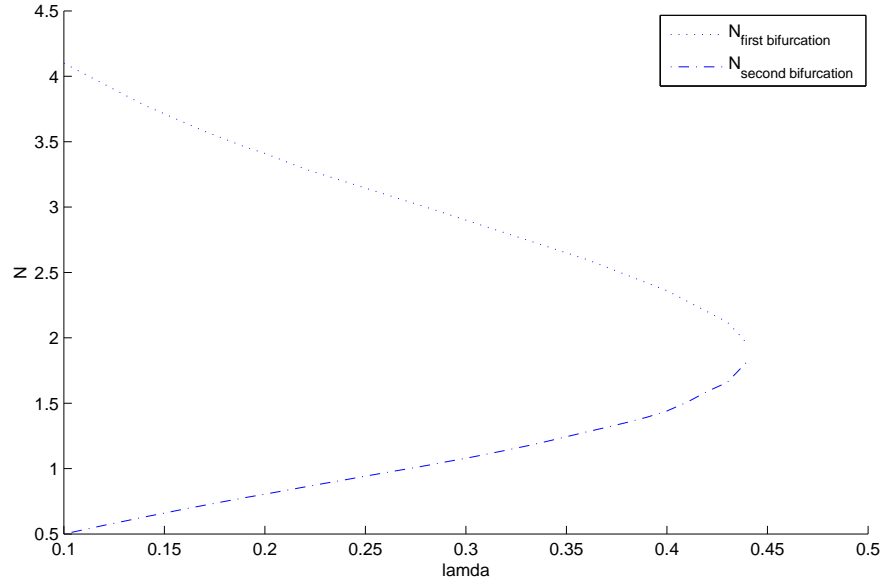


FIG. 4: Values of the norm (energy) of the symmetric soliton at which the direct and reverse bifurcations occur. The two curves merge and terminate at $\lambda = \lambda_{\max} \approx 0.44$.

complex eigenvalue(s)], which is indeed observed in the simulations (the validity of the VK criterion was not proved for the present model, but it was rigorously derived for another system, including two linearly coupled equations with the cubic nonlinearity of opposite signs [27]). On the other hand, inspection of dependences $N(k)$ for the asymmetric solutions demonstrates that, in all cases when these solitons are unstable, they have $dN/dk < 0$, i.e., they are expected to be VK-unstable solutions. The latter implies that the instability, being accounted for by a real eigenvalue, must grow without oscillations. The simulations support this expectation.

Stability of all solution branches which are shown as stable ones in Figs. 1 and 2 has also been verified in direct simulations. In all these cases, it was found that even relatively large perturbations do not destroy the solitons.

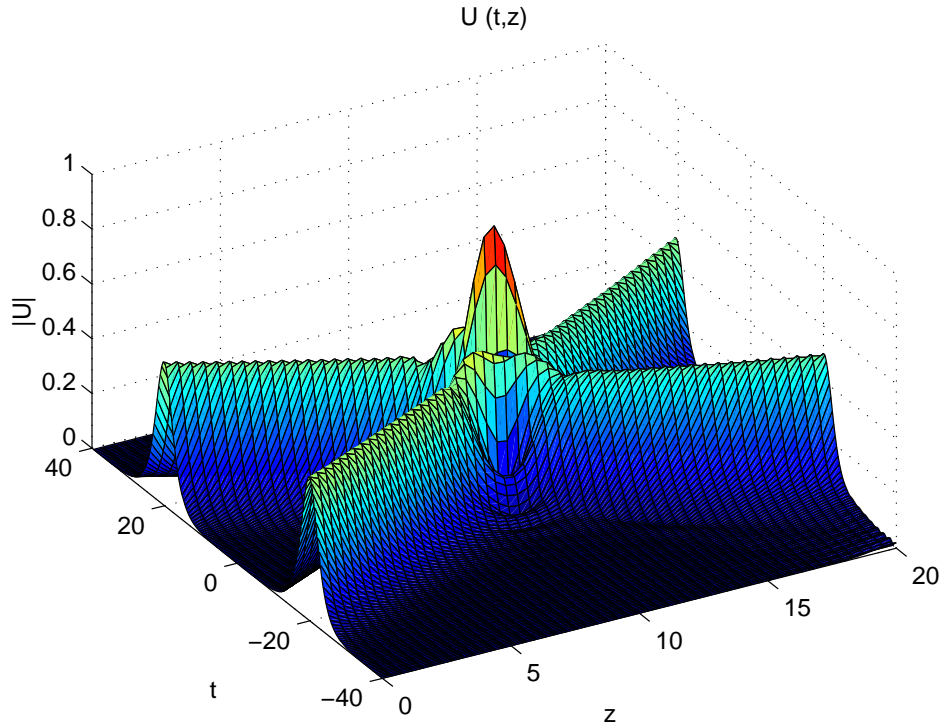


FIG. 5: A typical example of the elastic collision between two identical in-phase symmetric solitons generated by means of expressions (14) with $\chi = \pm 1$, for $\lambda = 0.32$ and $N = 1.106$ (which correspond to $k = 0.56$). Only the u -component is shown here, as the picture in the v -component is identical.

IV. COLLISIONS BETWEEN STABLE SOLITONS

The underlying system of Eqs. (1) and (2) is Galilean invariant: a “shove” transformation

$$\{u(\tau), v(\tau)\} \rightarrow \{u(\tau), v(\tau)\} e^{-i\chi\tau} \quad (14)$$

with an arbitrary real constant χ generates a *boosted* solution differing from the original one by $\tau \rightarrow \tau + 2\chi z$, i.e., it moves at the (inverse) velocity $c = -2\chi$ relative to the original state. The invariance suggests to study collisions between moving solitons (collisions between symmetric and asymmetric solitons in the model of a coupler with the cubic nonlinearity were investigated in Ref. [28]). Simulations of the collisions make it possible to draw the following general conclusions.

First, collisions between stable symmetric solitons (which are obviously tantamount to collisions between solitons in the single-component NLS equations with the CQ nonlinearity) appear to be completely elastic, as shown in Fig. 5. The elastic collisions give rise to small shifts of the solitons’ centers, in the same fashion as in collisions between solitons in the integrable cubic NLS equation (each soliton is additionally shifted in the direction of its motion).

Second, collisions between stable asymmetric solitons are essentially *inelastic*. In this case, the solitons emerge from the collision with smaller velocity c , and in an excited state, i.e., as *breathers*, rather than stationary solitons. For example, the (inverse) velocities of both solitons drop from $c_{\text{in}} = \pm 0.4$ before the collision to $c_{\text{out}} = \pm 0.2$ after the collision, if the moving solitons were generated by means of expression (14) with $\chi = \pm 0.2$, for $\lambda = 0.3$ and $N = 1.176$ (which correspond to $k = 0.6$).

The breathers which appear after the inelastic collision are not persistent ones. As Fig. 6 shows, the amplitude of the intrinsic oscillations of the breather gradually decreases, while the oscillation period increases. This may imply that, in the course of subsequent extended evolution, the breathers will eventually relax to stationary solitons (due to losses induced by emission of radiation), but detailed study of this stage of the evolution is beyond the scope of this work. It is noteworthy that, while the solitons generally keep their identity after the inelastic collision (the solitons which originally had a larger u - or v -component keep this difference after the collision), the post-collision oscillatory evolution clearly tends to *symmetrize* both pulses, so they may eventually settle down to a pair of identical symmetric solitons.

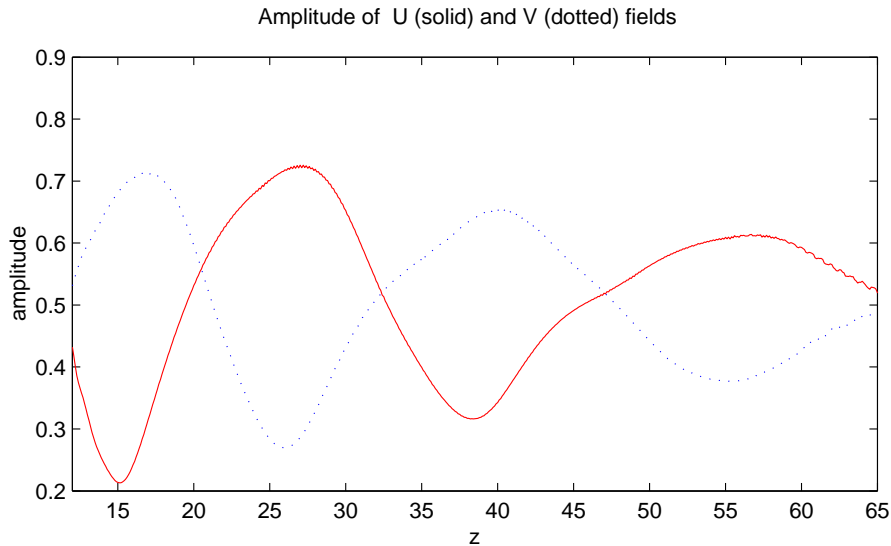


FIG. 6: The evolution of one of the breathers produced by the inelastic collision of two solitons in the above-mentioned example, with $\lambda = 0.3$, $N = 1.176$, $k = 0.6$, and shove parameters $\chi = \pm 0.2$ (the second breather is a mirror image of the one shown here). The solid and dashed curves show the amplitudes of the u - and v -components of the breather.

V. CONCLUSION

In this work, we have extended the model of the nonlinear dual-core coupler by adding defocusing quintic nonlinearity to the usual cubic self-focusing term. In terms of optics, the model may be interpreted in temporal and spatial domains alike (i.e., in fiber couplers and in a pair of tunnel-coupled parallel planar waveguides). As a result, at not too large values of the linear-coupling parameter λ , we observe a bifurcation loop for solitons: the supercritical bifurcation, which destabilizes the symmetric soliton and creates a pair of asymmetric ones, is followed by a reverse subcritical bifurcation that restores the stability of the symmetric soliton. In this case, the loop has the concave shape on its right side, and includes a large bistability region, which may be of interest for applications to all-optical switching. At larger values of λ , the loop's shape becomes convex, and the bistability disappears. At still larger λ , the symmetric solitons always remain stable, and asymmetric ones never appear.

The stability of all the branches of the soliton states, verified by direct simulations, exactly complies with what may be predicted, on the basis of the shape of the bifurcation diagrams, by general principles of the bifurcation theory. Additionally, in those cases when the asymmetric solitons are unstable, their instability is correctly predicted by the Vakhitov-Kolokolov criterion (while the instability of symmetric solitons has a different nature, as they are unstable against oscillatory perturbations). The simulations also demonstrate that unstable symmetric solitons rearrange themselves into stable asymmetric ones, with small radiation loss. Unstable asymmetric solitons rearranged into their still more asymmetric stable counterparts.

The Galilean invariance of the model makes it possible to study collisions between moving solitons. Symmetric solitons collide in a completely elastic fashion, while collisions between asymmetric solitons are inelastic: they lose, roughly, half of the velocity, and emerge from the collisions as breathers, that subsequently tend to symmetrize themselves and, possibly, settle down to stationary symmetric solitons.

It is plausible that basic results reported in this work are common to solitons in double-core systems with various forms of saturable nonlinearity. It may also be quite interesting to consider similar problems for two-dimensional solitons, that can be realized as spatiotemporal “light bullets” [19] in parallel-coupled planar waveguides with the intrinsic nonlinearity of the cubic-quintic type.

Appendix: Absence of asymmetric complex solitons generated by a bifurcation from the symmetric soliton

Here we aim to consider in more detail a possibility of the existence of stationary asymmetric soliton solutions in the complex form, as per Eqs. (5). Substituting the latter in the stationary version of Eqs. (1) and (2), one can easily

derive the following pair of equations,

$$\frac{d}{d\tau} \left(a^2 \dot{\phi} \right) = \lambda ab \sin(\phi - \psi), \quad \frac{d}{d\tau} \left(b^2 \dot{\psi} \right) = -\lambda ab \sin(\phi - \psi), \quad (15)$$

and another pair of equations, that we do not need here in an explicit form. An obvious consequence of Eqs. (15) for localized solutions, with $a(|\tau| = \infty) = b(|\tau| = \infty) = 0$, is relation (6).

If there is a bifurcation from the real symmetric soliton (3) that gives rise to complex asymmetric solitons with a nontrivial phase structure, then, in an infinitesimal proximity to the bifurcation point, where both the phase functions $\phi(\tau)$ and $\psi(\tau)$ and deviations of $a(\tau)$ and $b(\tau)$ from expression (3) are infinitely small, Eq. (6) yields, in the lowest-order approximation, $\dot{\phi} + \dot{\psi} = 0$, or, in other words, $\psi(\tau) = -\phi(\tau)$ (it is trivial to remove a phase constant). Further, in the same approximation, an equation for an infinitesimal function $\phi(\tau)$ following from Eqs. (15) is

$$-\frac{d^2 \phi}{dT^2} + 2\lambda a^4(T) \phi = 0, \quad (16)$$

where the expression (3) is to be substituted for a , and

$$T \equiv \int_0^\tau \frac{d\tau'}{a^2(\tau')} = \frac{1}{2(k-\lambda)} \left[\tau + \sqrt{\frac{1}{4(k-\lambda)}} - \frac{1}{3} \sinh(2\sqrt{k-\lambda}\tau) \right] \quad (17)$$

(T is a monotonous function of τ , varying together with it from $-\infty$ to $+\infty$). Equation (16) with $\lambda > 0$ is a linear Schrödinger equation with a coordinate T and potential *barrier* (rather than a potential well), which, obviously, gives rise to no localized eigenfunctions, hence it cannot generate any bifurcation that would be signalled by the appearance of such a solution (if one sets $\lambda < 0$, the conclusion will be the same, as in this case one will start with the antisymmetric soliton).

-
- [1] S. M. Jensen, IEEE J. Quant. Electr. **18**, 1580 (1982); A. M. Maier, Kvantovaya Elektron. (Moscow) **9**, 2296 (1982) [Sov. J. Quant. Electron. **12**, 1490 (1982)].
 - [2] E. M. Wright, G. I. Stegeman, and S. Wabnitz, Phys. Rev. A **40**, 4455 (1989).
 - [3] M. Romangoli, S. Trillo, and S. Wabnitz, Opt. Quantum Electron. **24**, S1237 (1992).
 - [4] I. M. Uzunov, R. Muschall, M. Göllés, Yu. S. Kivshar, B. A. Malomed, and F. Lederer, Phys. Rev. E **51**, 2527 (1995).
 - [5] C. Paré and M. Florjańczyk, Phys. Rev. A **41**, 6287 (1990).
 - [6] P. L. Chu, B. A. Malomed, and G. D. Peng, in *Proc. Seventeenth Austral. Conf. Opt. Fibre Technol.*, p. 266 (Institution of Radio and Electronics Engineers Australia, Hobart, 1992); J. Opt. Soc. Am. B **10**, 1379 (1993); N. Akhmediev and A. Ankiewicz, Phys. Rev. Lett. **70**, 2395 (1993).
 - [7] J. M. Soto-Crespo and N. Akhmediev, Phys. Rev. E **48**, 4710 (1993); N. Akhmediev and J. M. Soto-Crespo, Phys. Rev. E **49**, 4519 (1994).
 - [8] B. A. Malomed, I. Skinner, P. L. Chu, and G. D. Peng, Phys. Rev. E **53**, 4084 (1996).
 - [9] B. A. Malomed, Progr. Optics **43**, p. 71 (E. Wolf, editor: North Holland, Amsterdam, 2002).
 - [10] G. Iooss and D. D. Joseph, *Elementary Stability and Bifurcation Theory* (Springer-Verlag, New York, 1980).
 - [11] D. J. Kaup, T. I. Lakoba, and B. A. Malomed, J. Opt. Soc. Am. B **14**, 1199 (1997).
 - [12] T. I. Lakoba, D. J. Kaup, and B. A. Malomed, Phys. Rev. E **55**, 6107 (1997).
 - [13] W. C. K. Mak, B. A. Malomed, and P. L. Chu, J. Opt. Soc. Am. B **15**, 1685 (1998); Phys. Rev. E **69**, 066610 (2004).
 - [14] W. C. K. Mak, B. A. Malomed, and P. L. Chu, Phys. Rev. E **55**, 6134 (1997); Opt. Commun. **154**, 145 (1998).
 - [15] A. V. Buryak and A. A. Akhmediev, J. Opt. Soc. Am. B **11**, 804 (1994).
 - [16] A. Gubeskys and B. A. Malomed, Eur. Phys. J. D **28**, 283 (2004).
 - [17] F. Smektala, C. Quemard, V. Couderc, and A. Barthélémy, J. Non-Cryst. Solids **274**, 232 (2000); K. Ogusu, J. Yamasaki, S. Maeda, M. Kitao, and M. Minakata, Opt. Lett. **29**, 265 (2004).
 - [18] C. Zhan, D. Zhang, D. Zhu, D. Wang, Y. Li, D. Li, Z. Lu, L. Zhao, and Y. Nie, J. Opt. Soc. Am. B **19**, 369 (2002).
 - [19] B. A. Malomed, D. Mihalache, F. Wise, and L. Torner, J. Opt. B: Quant. Semics. Opt. **7**, R53 (2005).
 - [20] A. W. Snyder, D. J. Mitchell, L. Polodian, D. R. Rowland, and Y. Chen, J. Opt. Soc. Am. B **8**, 2102 (1991).
 - [21] S. Trillo, S. Wabnitz, G. I. Stegeman, and E. M. Wright, J. Opt. Soc. Am. B **6**, 889 (1989); R. S. Tasgal and B. A. Malomed, Phys. Scripta **60**, 418 (1999).
 - [22] B. J. Eggleton, R. E. Slusher, C. M. de Sterke, P. A. Krug, and J. E. Sipe, Phys. Rev. Lett. **76**, 1627 (1996); C. M. de Sterke, B. J. Eggleton, and P. A. Krug, J. Lightwave Technol. **15**, 1494 (1997).
 - [23] Kh. I. Pushkarov, D. I. Pushkarov, and I. V. Tomov, Opt. Quant. Electr. **11**, 471 (1979); S. Cowan, R. H. Enns, S. S. Rangnekar, and S. S. Sanghera, Can. J. Phys. **64**, 311 (1986).
 - [24] D. Mihalache, D. Mazilu, M. Bertolotti, and C. Sibilia, J. Opt. Soc. Am. B **5**, 565 (1988); D. Mihalache, M. Bertolotti, and C. Sibilia, Progr. Optics **27**, p. 229 (E. Wolf, editor: North Holland, Amsterdam, 1989).
 - [25] M. G. Vakhitov and A. A. Kolokolov, Izv. Vuz. Radiofiz. **16**, 1020 (1973) [in Russian; English translation: Sov. J. Radiophys. Quantum Electr. **16**, 783 (1973)].
 - [26] L. Bergé, Phys. Rep. **303**, 260 (1998).
 - [27] V. S. Shchesnovich, B. A. Malomed, and R. A. Kraenkel, Physica D **188**, 213 (2004).
 - [28] G. D. Peng, B. A. Malomed, and P. L. Chu, Phys. Scripta **58**, 149 (1998).